A Designed Four-α-Helix Bundle That Binds the Volatile General Anesthetic Halothane with High Affinity

Jonas S. Johansson,*† Daphna Scharf,*‡¶ Lowri A. Davies,‡¶ Konda S. Reddy,† and Roderic G. Eckenhoff*§
Departments of *Anesthesia, ‡Chemistry, and §Physiology, University of Pennsylvania; †Johnson Research Foundation; and ¶Center for Molecular Modeling, Philadelphia, Pennsylvania 19104 USA

ABSTRACT The structural features of volatile anesthetic binding sites on proteins are being examined with the use of a defined model system consisting of a four-α-helix bundle scaffold with a hydrophobic core. Previous work has suggested that introducing a cavity into the hydrophobic core improves anesthetic binding affinity. The more polarizable methionine side chain was substituted for a leucine, in an attempt to enhance the dispersion forces between the ligand and the protein. The resulting bundle variant has an improved affinity (K_d = 0.20 ± 0.01 mM) for halothane binding, compared with the leucine-containing bundle (K_d = 0.69 ± 0.06 mM). Photoaffinity labeling with ^{14}C-halothane reveals preferential labeling of the W15 residue in both peptides, supporting the view that fluorescence quenching by bound anesthetic reports both the binding energetics and the location of the ligand in the hydrophobic core. The rates of amide hydrogen exchange were similar for the two bundles, suggesting that differences in binding affinity were not due to changes in protein stability. Binding of halothane to both four-α-helix bundle proteins stabilized the native folded conformations. Molecular dynamics simulations of the bundles illustrate the existence of the hydrophobic core, containing both W15 residues. These results suggest that in addition to packing defects, enhanced dispersion forces may be important in providing higher affinity anesthetic binding sites. Alternatively, the effect of the methionine substitution on halothane binding energetics may reflect either improved access to the binding site or allosteric optimization of the dimensions of the binding pocket. Finally, preferential stabilization of folded protein conformations may represent a fundamental mechanism of inhaled anesthetic action.

INTRODUCTION

The mechanism of action of inhaled general anesthetics remains poorly understood (Franks and Lieb, 1994; Eckenhoff and Johansson, 1997). This situation results in part from the fact that the in vivo targets for these clinical agents are unknown, although membrane proteins that function as ion channels and/or neurotransmitter receptors in the central nervous system are currently in favor (Franks and Lieb, 1994; Harris et al., 1995). In support of this view are the studies demonstrating that the *activity* of both ligand-gated (Mihic et al., 1997; Jevtovic-Todorovic et al., 1998) and voltage-gated (Takenoshita and Steinbach, 1991) ion channels is modulated by inhalational general anesthetics. However, whether these changes in membrane protein function are attributable to direct effects of bound anesthetics or are instead an indirect result of changes in the physical properties of the lipid component of the plasma membrane (Cantor, 1997; Tu et al., 1998) remains to be determined.

A second obstacle to understanding mechanisms of anesthetic action has been the lack of methods that allow the investigator to *directly* monitor binding of these relatively weakly interacting ligands to proteins. However, techniques have been introduced in recent years that are based upon ^{19}F-NMR spectroscopy (Dubois and Evers, 1992; Dubois et al., 1993), direct photoaffinity labeling (Eckenhoff and Shuman, 1993), and fluorescence quenching (Johansson et al., 1995; Johansson, 1997), which allow the energetics of binding to be determined. The latter two techniques have the added advantage of providing information about the location of the bound anesthetic in the protein matrix. The demonstration of a direct interaction between anesthetic and protein is a crucial first step in understanding how these compounds might alter protein function.

The generic structural features of volatile anesthetic binding sites on proteins are being explored by use of a model system consisting of a four-α-helix bundle scaffold with a hydrophobic core (Johansson et al., 1996, 1998a; Johansson, 1998). The core can be modified using standard synthetic chemistry, allowing direct testing of the importance of both cavity size and potential amino acid side-chain electrostatic contributions to anesthetic binding. These synthetic peptide bundles are proposed to serve as scaled-down water-soluble models for the lipid-spanning domains of a number of structurally defined membrane proteins (Rees et al., 1989; von Heijne, 1994; Doyle et al., 1998). The rationale for this approach is supported by the evidence that the transmembrane portions of ligand-gated ion channels such as the $GABA_A$ receptor (Mihic et al., 1997) and the nicotinic acetylcholine receptor from *Torpedo nobiliana* (Eckenhoff, 1996a) may directly interact with volatile anesthetics.

In this paper, the design, synthesis, and initial characterization of a four-α-helix bundle that contains a relatively high-affinity binding site for halothane is reported. The location of the bound anesthetic was determined using both

Received for publication 23 March 1999 and in final form 28 October 1999.

Address reprint requests to Dr. Jonas Johansson, Department of Anesthesia, Hospital of the University of Pennsylvania, 780A Dulles, 3400 Spruce St., Philadelphia, PA 19104-4238. Tel.: 215-349-5472; Fax: 215-349-5078; E-mail: johansso@mail.med.upenn.edu.

0006-3495/00/02/982/12 $2.00

fluorescence quenching measurements and direct photoaffinity labeling, followed by microsequencing. The fluorescence quenching experiments and the direct photoaffinity labeling studies provide complementary information and reveal that the anesthetic indeed binds in the designed cavity in the hydrophobic core of the four-α-helix bundle. In addition, the structural and dynamic properties of the four-α-helix bundle are examined using molecular dynamics (MD) computer simulations.

MATERIALS AND METHODS

Materials

9-Fluorenylmethoxycarbonyl (Fmoc)-protected amino perfluorophenyl esters were purchased from PerSeptive Biosystems (Framingham, MA), with the exception of 9-fluorenylmethoxycarbonyl-L-Arg(2,2,5,7,8-pentamethylchroman-6-sulfonyl)-pentafluorophenyl ester (Fmoc-L-Arg(Pmc)- Opfp), which was obtained from Bachem (King of Prussia, PA). Halothane (2-bromo-2-chloro-1,1,1-trifluoroethane) was from Halocarbon Laboratories (Hackensack, NJ). The thymol preservative present in commercial halothane was removed with an aluminum oxide column (Shibata et al., 1991). [^{14}C]Halothane ([1-^{14}C]-2-bromo-2-chloro-1,1,1-trifluoroethane; 50 mCi/mmol) was purchased from DuPont NEN (Boston, MA). Guanidinium chloride (GndCl) (8.0 M) was obtained from Pierce (Rockford, IL). Hexane and 2,2,2-trifluoroethanol (TFE) (NMR grade) were from Aldrich Chemical Co (Milwaukee, WI). All other chemicals were of reagent grade and were purchased from Sigma Chemical Co. (St. Louis, MO).

Peptide synthesis and preparation

Peptides were assembled on NovaSyn PR-500 resin (Novabiochem, La Jolla, CA), using the Fmoc/*tert*-butyl (Fmoc/^{t}Bu) protection strategy on a Milligen 9050 (Cambridge, MA) instrument (Robertson et al., 1994; Rabanal et al., 1996; Gibney et al., 1997a; Johansson et al., 1998a,b; Johansson, 1998). Reversed-phase C_{18} high-performance liquid chromatography (HPLC) with aqueous acetonitrile gradients containing 0.1% (v:v) trifluoroacetic acid was used to purify crude peptides to homogeneity. Peptide identities were confirmed with laser desorption mass spectrometry. Solution molecular weights were determined with gel filtration on a Superdex 75 FPLC column (Pharmacia Biotechnology, Piscataway, NJ), using the following molecular mass standards: aprotinin (6.5 kDa), cytochrome *c* (12.4 kDa), chymotrypsinogen A (25.0 kDa), carbonic anhydrase (29.0 kDa), ovalbumin (43.0 kDa), and bovine serum albumin (67.0 kDa).

Circular dichroism spectroscopy

Spectra were recorded on a model 62 DS spectropolarimeter (Aviv, Lakewood, NJ), using 2-mm pathlength quartz cells. The cell holder was temperature controlled at 25.0 ± 0.1°C. The buffer was 10 mM potassium phosphate at pH 7.0. The bandwidth was 1.00 nm, with a scan step of 0.5 nm and an average scan time of 3.0 s.

Denaturation studies

Denaturation of four-α-helix bundles was followed using circular dichroism (CD) spectroscopy, monitoring the ellipticity at 222 nm (Θ_{222}), as described (Johansson et al., 1998a). The measured Θ_{222} as a function of the added denaturant concentration was fit to the equation of Mok et al. (1996) describing the unfolding of a dimer (four-α-helix bundle) into two monomers, using a nonlinear least-squares routine,

$$\text{Fraction folded} = 1 - [[\exp(\Delta G^{H_2O} + m \cdot [\text{denaturant}])]/R \cdot T] \div [4 \cdot P(1 + (8 \cdot P/(\exp(\Delta G^{H_2O} + m \cdot [\text{denaturant}])/R \cdot T)) - 1)^{1/2}], \quad (1)$$

where ΔG^{H_2O} is the conformational stability of the protein, m is the slope of the unfolding transition, [denaturant] is the molar concentration of GndCl, R is the gas constant, T is the absolute temperature, and P is the molar monomer concentration of the protein.

Steady-state fluorescence measurements

Binding of halothane to the current four-α-helix bundle designs was determined by using steady-state intrinsic tryptophan fluorescence measurements (Johansson et al., 1995, 1996, 1998a) on a K2 multifrequency cross-correlation phase and modulation spectrofluorometer (ISS, Champaign, IL). Tryptophan was excited at 280 nm (bandwidth 2 nm), and emission spectra (bandwidth 8 nm) were recorded with peaks at 327 nm for (DesAc-Aα_2)$_2$ (peptide lacking an N-terminus acetyl group) and 323 nm for (DesAc-Aα_2-L38M)$_2$. A 305-nm emission cut-on filter was used to minimize the transmission of scattered excitation light. The quartz cell had a path length of 10 mm and a teflon stopper. The cell holder was thermostatically controlled at 25.0 ± 0.1°C. The buffer used for the fluorescence experimentation was 130 mM NaCl, 20 mM sodium phosphate (pH 7.0). Protein concentrations were determined with a UV/Vis Spectrometer Lambda 2 (Perkin-Elmer, Norwalk, CT), taking ϵ_{280} for tryptophan = 5700 M^{-1} cm^{-1} (Edelhoch, 1967). Halothane-equilibrated bundle proteins, in gas-tight Hamilton syringes (Reno, NV), were diluted with predetermined volumes of plain protein (not exposed to anesthetic, but otherwise treated in the same manner) to achieve the final anesthetic concentrations indicated in the figures.

As described previously (Johansson et al., 1995, 1996, 1998a), the quenched fluorescence (Q) is a function of the maximum possible quenching (Q_{max}) at an infinite halothane concentration ([Halothane]) and the affinity of halothane for its binding site (K_d) in the vicinity of the tryptophan residues. From mass law considerations, it then follows that

$$Q = (Q_{max} \cdot [\text{Halothane}])/(K_d + [\text{Halothane}]). \quad (2)$$

Photoaffinity labeling and sequencing

Deoxygenated four-α-helix bundle solutions (7 μM in 50 mM sodium phosphate, pH 7.0) containing 0.2 mM [^{14}C]halothane (50 mCi/mmol) were exposed to 254-nm light (mercury pencil calibration lamp; Oriel, Stratford, CT) for 60 s in 5-mm-path length quartz cuvettes at room temperature, with constant stirring. Peptides were washed and concentrated using 3-kDa molecular mass cutoff filters (Amicon, Beverly, MA) and then sequenced directly on an Applied Biosystems (Foster City, CA) model 473A sequencer. Small-scale analytical runs (50 pmol) confirmed the expected identity and release pattern for the first three residues. Radioactivity release was then obtained using pre-HPLC samples from ~2 nmol peptide load.

Hydrogen exchange

Peptides (3–5 mg) were dissolved in 1 ml of 1 M guanidinium chloride and 50 mM sodium phosphate (pH 8.5), with 40 μl ^{3}HOH added (100 mCi/ml; ICN, Costa Mesa, CA), and allowed to equilibrate overnight at 20°C to permit complete exchange-in of tritium. The peptide solutions were then

passed through a PD-10 gel filtration column (Sigma Chemical Co.) to remove free ^{3}HOH and to switch to the exchange-out buffer, 50 mM sodium phosphate (pH 7.0). The protein fraction was collected and immediately placed in gas-tight Hamilton syringes prefilled with exchange-out buffer, with or without 4 mM halothane. The syringe contents were mixed with microstir bars, and 100-μl aliquots were precipitated with 2 ml 20% trichloroacetic acid (TCA) at regular intervals, immediately filtered through Whatman (Hillsboro, OR) GF/F filters, and washed with 8 ml 2% TCA. Filters were equilibrated with 10 ml fluor overnight and counted with the use of liquid scintillation. Parallel aliquots allowed determination of protein concentration, using UV/Vis absorption spectroscopy at 280 nm.

Protection factors for given hydrogens were determined from the exchange-out curves (Fig. 8). Assuming the horizontal equivalence of hydrogen exchange (the nth hydrogen to exchange is the same with and without anesthetic), protection factor ratios were estimated by dividing the time required for a given hydrogen to exchange under differing conditions (i.e., with and without anesthetic) and were determined for the last hydrogens in common for the two conditions. Protection factor ratios (Pfrs) were averaged, and $\Delta\Delta G$ values (the change in the free energy favoring the folded conformation) were determined, using the relationship $\Delta\Delta G = -RT\ln(\text{Pfr})$, where R is the gas constant and T is the absolute temperature. Negative values reflect the stabilization of the native folded conformation (slower exchange), and positive values indicate destabilization (faster exchange).

Molecular dynamics simulations

The equilibrium structures of the solvated four-α-helix bundles (Ac-Aα_2)$_2$ and (Ac-Aα_2-L38M)$_2$ were obtained (Davies et al., 1999a) with a state-of-the-art MD program (Martyna et al., 1996). Initial coordinates for the Ac-Aα_2 monomer were generated with InsightII software (Molecular Simulations, San Diego, CA), following the primary sequence, secondary structure domains, and relative residue orientations reported (Johansson et al., 1998a). Two such monomers were placed in an *anti* topology such that the residues, which occupy the a and d heptad positions, formed the hydrophobic core. An aqueous environment for the (Ac-Aα_2)$_2$ four-α-helix structure was created by immersion in a box containing ~6700 water molecules, ensuring that no overlap existed between water molecules and peptide. The AMBER95 force field and parameters (Weiner et al., 1984, 1986; Cornell et al., 1995) were used to describe the peptide interactions, and the TIP3P potential (Jorgensen et al., 1983) was used for the water molecules.

After local minimization of the four-α-helix bundle structure, MD equilibration of the solvated peptide was performed: 300 ps at a constant temperature of 25°C, with a constant simulation box volume, followed by 1 ns at a constant pressure of 1 atmosphere, at the same temperature. The averaged structure for (Ac-Aα_2)$_2$ in water was calculated over the last 500 ps of the MD constant-pressure trajectory. Coordinates for the (Ac-Aα_2-L38M)$_2$ structure were obtained by substituting the L38 residue with M38 in the averaged configuration of (Ac-Aα_2)$_2$, using InsightII. This (Ac-Aα_2-L38M)$_2$ structure was similarly solvated in a water box and minimized, before MD equilibration was carried out for 300 ps at a constant temperature (25°C) and volume, followed by a 300-ps trajectory at a constant pressure (1 atmosphere), at the same temperature. Averaged structures for both four-α-helix bundles were obtained using the last 100 ps of the constant-pressure MD trajectories.

A single halothane molecule was placed in the hydrophobic pocket of the equilibrated (Ac-Aα_2-L38M)$_2$ structure. Initial coordinates for the anesthetic were generated with InsightII software. After minimization, MD equilibration was performed for 300 ps, as above.

Gas chromatography

Buffer concentrations of halothane were determined, using gas chromatography, with an HP 6890 series instrument (Hewlett Packard, Wilmington, DE), as described (Johansson et al., 1996).

Curve fitting and statistics

Best-fit curves were generated with the KaleidaGraph (Abelbeck Software, Reading, PA, 1994) program. Data are expressed as means ± SD or SEM.

RESULTS

Protein design

The overall four-α-helix bundle scaffold (Fig. 1) was designed to be water soluble and to have a hydrophobic core as described (Robertson et al., 1994; Rabanal et al., 1996; Gibney et al., 1996, 1997a,b). The bundles examined in this study were based on prior designs (Gibney et al., 1996, 1997a,b) and were constructed from two 62-residue di-α-helical peptides (Fig. 1), each composed of two 27-residue amphiphilic α-helical segments and an eight-residue flexible glycine linker. The bundle designs have two tryptophan residues (W15) at hydrophobic heptad a positions (Fig. 2). The primary sequences of the two 62-residue di-α-helical peptides that are the focus of the current study are presented in Fig. 2 *a*. The peptides described are designated DesAc-Aα_2, which is a variant of the Ac-Aα_2 peptide reported previously (Johansson et al., 1998a) that lacks the N-terminus acetyl group, and DesAc-Aα_2-L38M, which has a methionine in place of a leucine at position 38 (a heptad e position). The N-termini acetyl groups were omitted to allow peptide microsequencing. The solution NMR structure of the four-α-helix bundle that served as a starting point for the current bundle designs (Gibney et al., 1997b) suggests that the 38 heptad e position is part of the hydrophobic core (Skalicky et al., 1999).

In an effort to further our understanding of the structural make-up of volatile anesthetic binding sites in proteins, we introduced a potential electrostatic interaction in the vicinity of the designed hydrophobic core cavity (Johansson et al.,

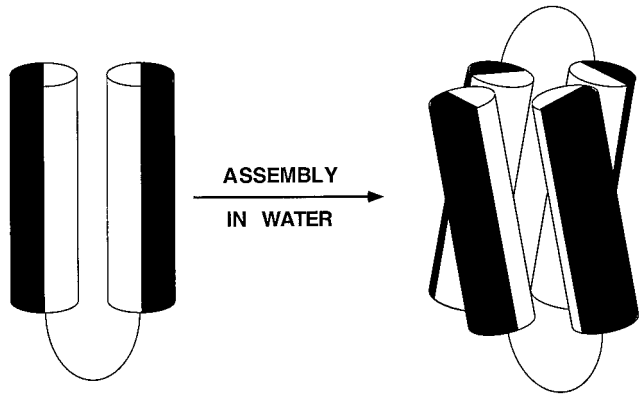

FIGURE 1 Modeled structure of the synthetic four-α-helix bundles. The cylinders represent the two 27-residue amphiphilic α-helical portions of each 62-residue di-α-helical peptide, joined by an eight-residue glycine linker. Black and white halves of each cylinder represent hydrophilic and hydrophobic residues, respectively. Di-α-helical peptides dimerize in water to form four-α-helix bundles.

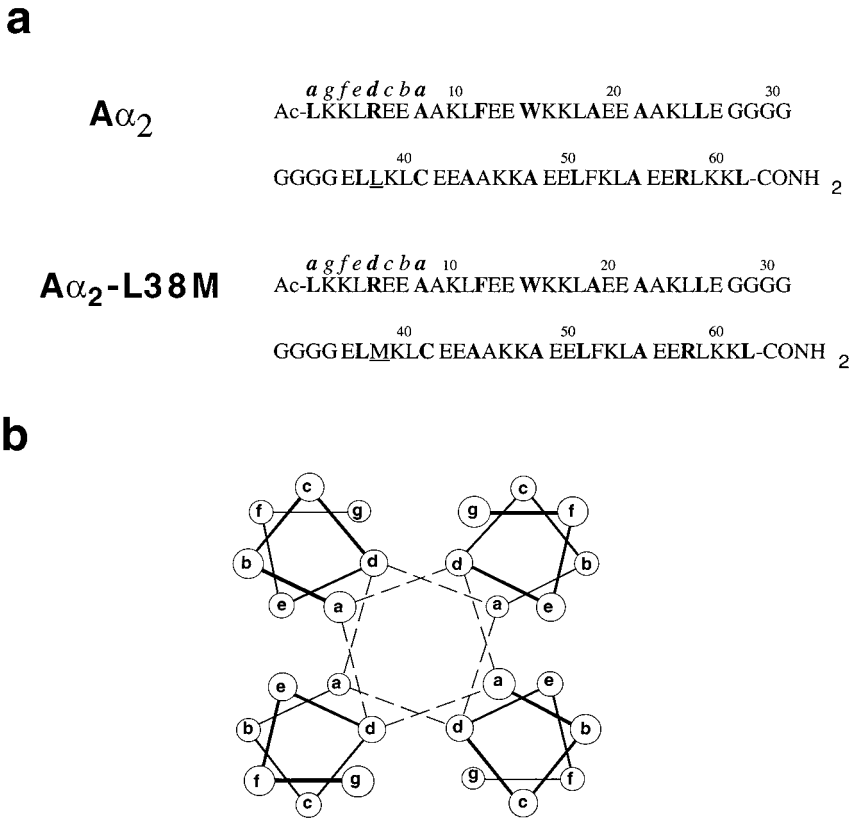

FIGURE 2 (*a*) Primary sequences of the $(\text{DesAc-A}\alpha_2)_2$ and $(\text{DesAc-A}\alpha_2\text{-L38M})_2$ di-α-helical peptides, with hydrophobic heptad a and d residues shown in bold. The C-termini have carboxyamide groups. The heptad repeat assignments (abcdefg) used to design amphiphilic α-helices are shown above the initial amino acids of each di-α-helical peptide. (*b*) End-on view of *anti* four-α-helix bundle, showing the interaction of the hydrophobic core residues at the heptad a and d positions. The dashed lines indicate how successive hydrophobic core layers are composed of two a and two d residues. Modified from Betz et al. (1997).

1998a) by replacing a heptad e position leucine with a methionine to form $(\text{DesAc-A}\alpha_2\text{-L38M})_2$. Methionine was selected because it is similar to leucine in terms of size (both residues have side-chain volumes of 124 Å^3; Richards, 1974), helix-forming propensity (O'Neil and DeGrado, 1990a), and hydrophobicity (Nozaki and Tanford, 1971; Urry et al., 1992; Wimbley and White, 1996) but contains the more polarizable sulfur atom, which potentially provides energetically more favorable interactions with a bound hydrophobic ligand (Fersht and Dingwall, 1979; Gellman, 1991). A tryptophan occupies a position at one end of the putative cavity (W15; Fig. 2 *a*) to permit protein concentration determination (Edelhoch, 1967) and to allow monitoring of anesthetic binding (Johansson et al., 1995, 1996, 1998a; Johansson, 1997, 1998). In addition, the tryptophan residue may provide a weak electrostatic contribution to the overall anesthetic binding energetics (Dougherty, 1996; Eckenhoff and Johansson, 1997).

α-Helical content and conformational stabilities of the four-α-helix bundles $(\text{DesAc-A}\alpha_2)_2$ and $(\text{DesAc-A}\alpha_2\text{-L38M})_2$

CD spectroscopy was used to measure the α-helical content of the four-α-helix bundles $(\text{DesAc-A}\alpha_2)_2$ and $(\text{DesAc-A}\alpha_2\text{-L38M})_2$ and to evaluate the effect of removing the capping acetyl group from the N-terminus. Table 1 shows that the $-[\Theta]_{222}$ (in deg cm^2 dmol^{-1}) of $(\text{DesAc-A}\alpha_2)_2$ and $(\text{DesAc-A}\alpha_2\text{-L38M})_2$ is 22,000 and 21,600, respectively. For comparison the $-[\Theta]_{222}$ of the N-capped $(\text{Ac-A}\alpha_2)_2$ bundle is 23,000 deg cm^2 dmol^{-1}. The measured $-[\Theta]_{222}$

TABLE 1 Spectral and thermodynamic properties of the four-α-helix bundles $(\text{DesAc-A}\alpha_2)_2$, $(\text{DesAc-A}\alpha_2\text{-L38M})_2$, and $(\text{A}\alpha_2)_2$

Four-α-Helix Bundle	Solution Molecular Mass (kDa)	Fluorescence Maximum (nm)	ΔG^{H_2O} (kcal/mol)	m (kcal/mol M)	$-[\Theta]_{222}$ (deg cm^2 dmol^{-1})	Halothane K_d (μM)
$(\text{DesAc-A}\alpha_2)_2$	13.2	327	11.5 ± 0.3	1.8 ± 0.1	22,000	690 ± 60
$(\text{DesAc-A}\alpha_2\text{-L38M})_2$	14.9	323	11.7 ± 0.2	2.0 ± 0.1	21,600	200 ± 10
$(\text{A}\alpha_2)_2$	18.5	327	14.3 ± 0.8	2.0 ± 0.2	23,000	710 ± 40

Data for $(\text{A}\alpha_2)_2$ are taken from Johansson et al. (1998a), except for the solution molecular mass, which was redetermined using a different column described under Materials and Methods.

values for (DesAc-Aα_2)$_2$ and (DesAc-Aα_2-L38M)$_2$ translate into percentage α-helical contents of 79.0% and 77.3%, respectively, using a value of 32,000 deg cm^2 dmol^{-1} for 100% α-helix (Lau et al., 1984). Removal of the N-termini acetyl groups therefore results in a 4–5% decrease in α-helical content.

The conformational stabilities of the two four-α-helix bundles (DesAc-Aα_2)$_2$ and (DesAc-Aα_2-L38M)$_2$ were determined using chemical denaturation with GndCl. The ellipticity at 222 nm for the four-α-helix bundles was measured as a function of added denaturant, and the data were fit using Eq. 1. Fig. 3 shows that both (DesAc-Aα_2)$_2$ and (DesAc-Aα_2-L38M)$_2$ undergo full denaturation in the presence of GndCl. The calculated ΔG^{H20} and m values for the two four-α-helix bundles are given in Table 1. Removal of the two N-termini acetyl groups leads to a ~3 kcal/mol destabilization of both four-α-helix bundles compared to the parent bundle (Ac-Aα_2)$_2$, in line with the 1–2 kcal/mol α-helix stabilizing effect attributed to the presence of a single N-capping group (Bryson et al., 1995).

Location of Met^{38}

The solution NMR structure of the four-α-helix bundle (Gibney et al., 1997b) that served as an initial model for the current bundle designs revealed that the 38 heptad e position residue (a tryptophan) is located in the hydrophobic core (Skalicky et al., 1999). The fluorescence yields of the W15 residues in the two current bundles (DesAc-Aα_2)$_2$ and (DesAc-Aα_2-L38M)$_2$ were compared to determine whether the methionine at position 38 formed part of the hydrophobic core. Methionine will quench the tryptophan fluorescence (Ballew et al., 1996) if the sulfur atom is located within 7 Å of the indole ring (Yuan et al., 1998). Fig. 4 shows that the W15 fluorescence yield of the (DesAc-Aα_2-L38M)$_2$ bundle is 67–73% (n = 2) of that displayed by the (DesAc-Aα_2)$_2$ bundle, indicating that the methionine side chain is located in the vicinity of W15.

Binding of the volatile anesthetic halothane to the hydrophobic cores of the four-α-helix bundles

The binding of halothane to the four-α-helix-bundle (DesAc-Aα_2-L38M)$_2$ hydrophobic core was followed by tryptophan fluorescence quenching (Johansson et al., 1995, 1996, 1998a), as shown in Fig. 5. Halothane causes a concentration-dependent quenching of the intrinsic W15 fluorescence, without changing the emission maximum, indicating that halothane binds in the vicinity of the indole rings without altering the local dielectric environment. Furthermore, the lack of a red shift in the tryptophan fluorescence emission maximum upon halothane binding suggests that the anesthetic does not promote unfolding of the bundle, which would lead to increased water exposure of the indole rings. Fig. 6 *a* shows a plot of the bundle tryptophan fluorescence as a function of the halothane concentration. Fitting the data with Eq. 2 yields a K_d = 0.20 ± 0.01 mM with a Q_{max} = 0.98 ± 0.01, indicating that the fluorescence of both of the tryptophan residues in the bundle core is quenched by bound anesthetic. For comparison, Fig. 6 *b* shows the measured binding of halothane to the hydrophobic core of the bundle (DesAc-Aα_2)$_2$. The calculated binding parameters are K_d = 0.69 ± 0.06 mM and Q_{max} = 0.97 ± 0.02, again implying that the fluorescence of both tryptophan residues is quenched. The affinity of halothane binding to the (DesAc-Aα_2-L38M)$_2$ is increased as compared to the (DesAc-Aα_2)$_2$ bundle, by a factor of 3.5.

The importance of bundle tertiary structural interactions for anesthetic binding is shown in Fig. 6 *c*, which demonstrates the diminished quenching of W15 fluorescence in the

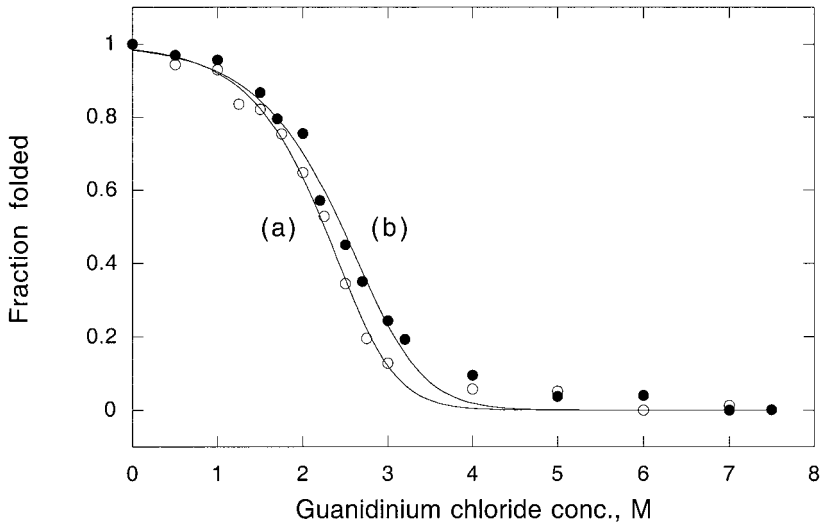

FIGURE 3 Four-α-helix bundle denaturation curves as monitored by spectropolarimetry at 222 nm. (*a*) (DesAc-Aα_2)$_2$. (*b*) (DesAc-Aα_2-L38M)$_2$. The ΔG^{H20} and m values calculated with Eq. 1 are given in Table 1.

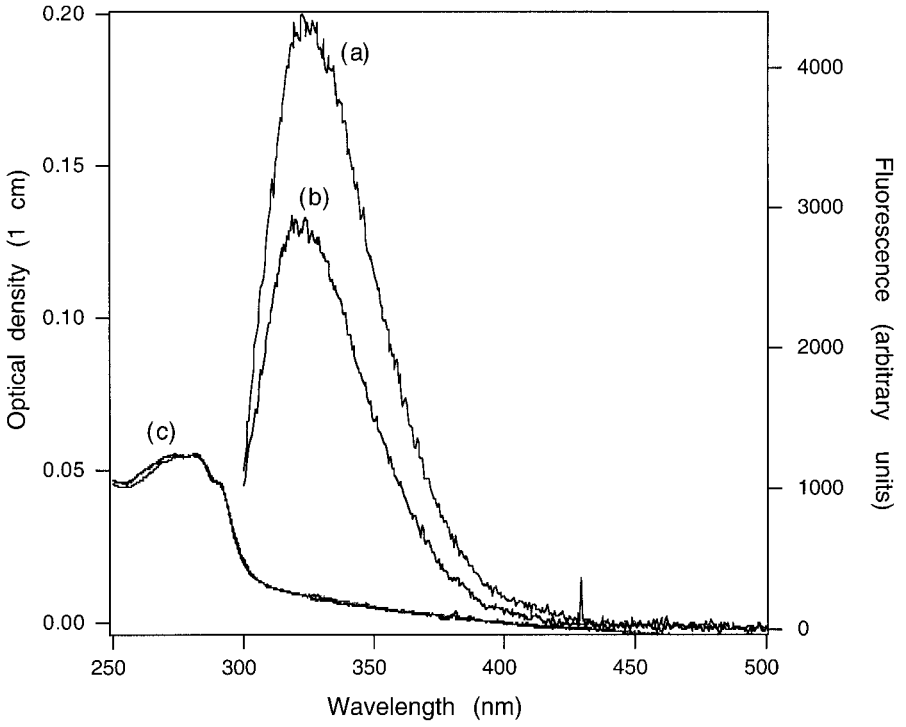

FIGURE 4 Relative W15 fluorescence yields of the four-α-helix bundles (DesAc-Aα_2)$_2$ (*a*) and (DesAc-Aα_2-L38M)$_2$ (*b*). In both cases, the peptide concentration was 4.8 μM, as shown by the absorption spectra in *c*. Excitation was at 280 nm, with emission maxima at 327 and 323 nm for the (DesAc-Aα_2)$_2$ and (DesAc-Aα_2-L38M)$_2$ bundles, respectively.

(DesAc-Aα_2-L38M)$_2$ bundle by halothane after bundle dissociation with TFE. TFE negates the hydrophobic interactions that underlie four-α-helix bundle formation (Zhou et al., 1992), while maintaining secondary structure (Jasanoff and Fersht, 1994). The magnitude of fluorescence quenching in 50% TFE is comparable to that measured when halothane is added to *free* L-tryptophan in solution (Johansson et al., 1995, 1996, 1998a) and results from collisional encounters between halothane and the dissociated di-α-helical peptides.

Photoaffinity labeling and microsequencing of the four-α-helix bundles

After exposure to 60 s of UV light, both peptides had incorporated label at an approximate stoichiometry of 1:1 bundle. Exposing the (DesAc-Aα_2-L38M)$_2$ bundle to a denaturing GndCl concentration (2 M; Fig. 3) resulted in much less label incorporation (0.07:1 bundle), compatible with specific labeling of the native four-α-helix bundle structure. Microsequencing revealed the expected initial five residues

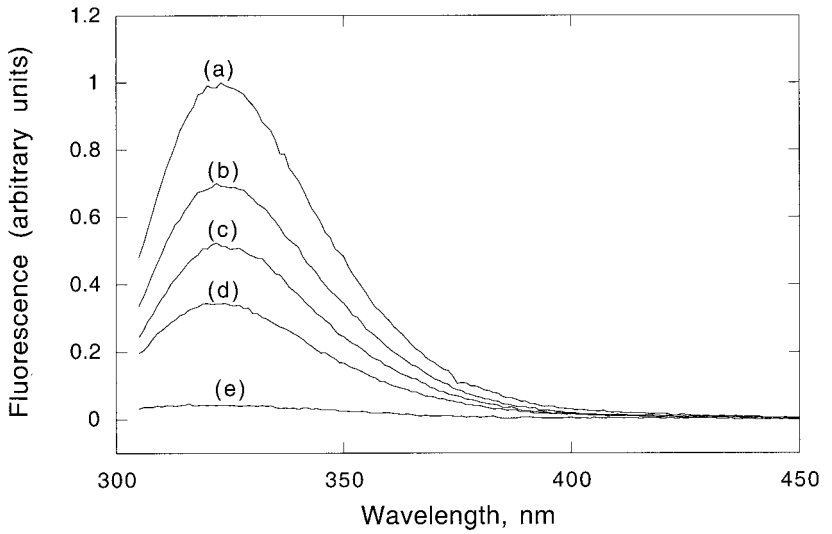

FIGURE 5 Quenching of the (DesAc-Aα_2-L38M)$_2$ bundle (5 μM) W15 fluorescence by halothane. Excitation was at 280 nm, with the emission maximum at 323 nm. The concentrations of halothane were (*a*) 0, (*b*) 72, (*c*) 142, (*d*) 250, and (*e*) 5000 μM. The fluorescence intensity has been normalized.

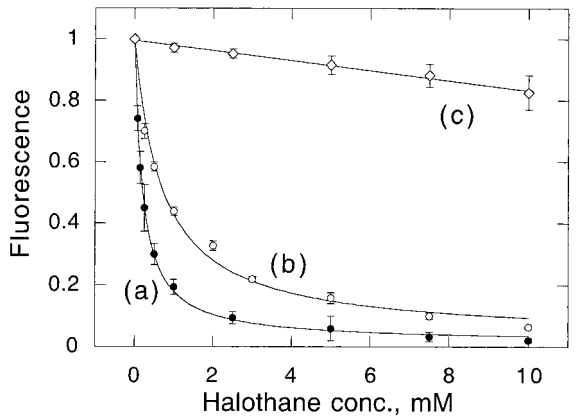

FIGURE 6 Comparison of quenching profiles for the two four-α-helix bundles (DesAc-Aα_2-L38M)$_2$ (*a*) and (DesAc-Aα_2)$_2$ (*b*) by added halothane. The bundle protein concentration was 5 μM. Data points are the means of three to six experiments on separate samples; error bars represent the SD. The lines through the data points have the form of Eq. 2. (*c*) Effect of halothane on (DesAc-Aα_2-L38M)$_2$ W15 fluorescence in the presence of 50% (6.9 M) TFE.

from both bundles (LKKLR) with approximately the same recovery from analytical samples. Larger samples (2 nmol) were sequenced for 30 cycles (about half-way through the peptide), and pre-HPLC recovery revealed the cpm shown in Fig. 7 *a*. The (DesAc-Aα_2)$_2$ bundle released a small number of counts along with the E6, A8, and F12 residues, but the dominant release occurred coincidentally with the W15 residue (Fig. 7 *b*). The W15:F12 release ratio was ~8 for the (DesAc-Aα_2)$_2$ peptide. The (DesAc-Aα_2-L38M)$_2$ peptide also had minor release at the E6 and F12 positions, but a much more pronounced release at the W15 cycle. In the case of (DesAc-Aα_2-L38M)$_2$, the W15:F12 release ratio was 50. For comparison, labeling of the (DesAc-Aα_2-L38M)$_2$ bundle in the presence of a denaturing GndCl concentration (2 M) resulted in the release of only one-sixth of the counts associated with the folded bundle, and there was no detectable release on the F12 cycle.

Effect of bound halothane on the dynamics of the four-α-helix bundles

Fig. 8 shows that terminal hydrogen exchange rates for the two four-α-helix bundles was comparable, consistent with the similar stability estimates derived from the GndCl denaturation experiments (Table 1). Because these terminal hydrogens exchange in ~100 min (6000 s), and freely exposed amide hydrogens exchange in ~0.1 ms, protection factors can be estimated to have values of 6×10^5. Assuming that these slow hydrogens exchange only through global unfolding events, the stability of the four-α-helix bundles is estimated to be ~8 kcal/mol, somewhat less than that measured by the GndCl denaturation experiments using CD spectroscopy. This is not unexpected, because 1) hydrogen exchange probes the stability of tertiary and quarternary structure in this dimeric peptide, whereas the GndCl denaturation experiments as followed by CD spectroscopy probe secondary structure, and it is not clear how cooperative the unfolding event is in these peptides (*m* values in Table 1), and 2) the slow hydrogens in these peptides may exchange through pathways involving incomplete unfolding events.

More importantly, the folded conformation of both bundles was stabilized in the presence of halothane. Thus halothane stabilized the (DesAc-Aα_2)$_2$ and (DesAc-Aα_2-L38M)$_2$ bundles by -0.7 and -0.9 kcal/mol, respectively, consistent with the premise of preferential binding to the folded dimeric bundle. The difference in halothane-induced stabilization on the order of 0.2 kcal/mol implies a difference in K_d values for halothane binding for the two bundles of ~1.4, somewhat less than the 3.5-fold difference found using fluorescence quenching to monitor anesthetic binding. However, the overall agreement in both direction and magnitude is reasonable when one considers the global versus regional nature of the two approaches for determining anesthetic binding to the four-α-helix bundles.

Molecular dynamics simulations of the four-α-helix bundles

Molecular dynamics (MD) simulations were carried out to begin to understand how the position 38 residue (leucine versus methionine) might play a role in anesthetic binding. The predominant α-helical nature of the peptide backbone is maintained during the simulation for both solvated (Ac-Aα_2)$_2$ and (Ac-Aα_2-L38M)$_2$ four-α-helix bundles, in agreement with the experimental results. The individual helices were observed to undergo bending and twisting during the equilibration. The hydrophobic heptad a and d position residues remain buried within the core of the four-α-helix bundles, with the exception of the positively charged arginine residues (R5 and R58) near both termini, in agreement with the solution NMR structure of a closely related four-α-helix bundle (Skalicky et al., 1999).

The mean square displacements of the terminal methyl carbon atoms in residue 38 with respect to the C_α atom were monitored during the simulations. The side chain of M38 in the (Ac-Aα_2-L38M)$_2$ four-α-helix bundle was observed to be more mobile than the L38 side chain in (Ac-Aα_2)$_2$, which is in good agreement with experimental data (Gellman, 1991).

Both (Ac-Aα_2)$_2$ and (Ac-Aα_2-L38M)$_2$ four-α-helix bundles exhibit a hydrophobic pocket that can bind at least one halothane molecule. A snapshot taken from the initial phase of equilibration of the solvated (Ac-Aα_2-L38M)$_2$ bundle with halothane is shown in Fig. 9. The distance between the sulfur atom of M38 and the indole ring of W15 is such that a halothane molecule can be accommodated. Therefore, it is plausible that a single halothane molecule, which exhibits end-on-end rotational and translational motions in the

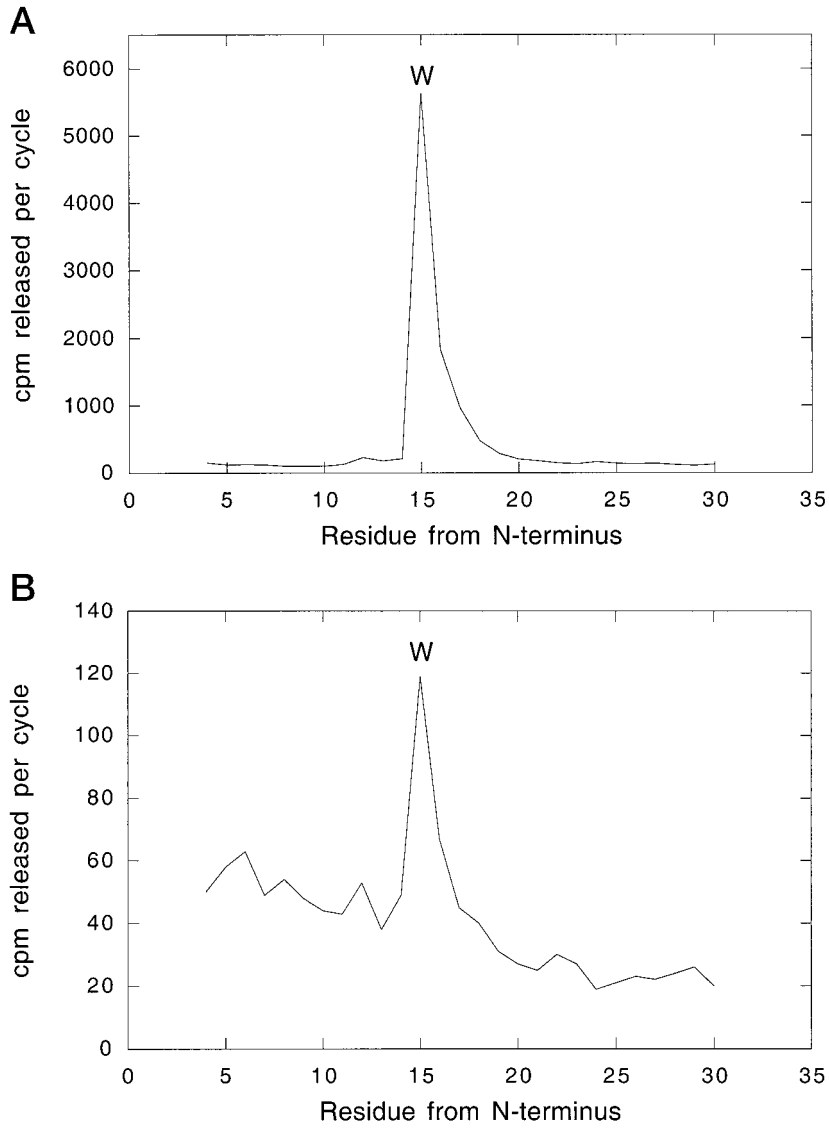

FIGURE 7 Disintegrations per cycle after microsequencing of the (*a*) (DesAc-Aα_2-L38M)$_2$ and (*b*) (DesAc-Aα_2)$_2$ four-α-helix bundle. Letters are standard amino acid abbreviations.

pocket, can satisfy the spatial requirements for fluorescence quenching, especially since the side chains of M38 and W15 are also mobile.

DISCUSSION

The in vivo sites of volatile anesthetic action remain to be determined, although membrane proteins in the central nervous system are currently argued to be likely targets (Franks and Lieb, 1994; Harris et al., 1995). The three-dimensional structures of most ligand-gated ion channels, including those thought to be important for anesthetic action, are not yet clear. However, the transmembrane domains are believed to be composed of bundles of α-helices, based upon the few crystal structures available for other types of membrane proteins (Rees et al., 1989; von Heijne, 1994; Doyle et al., 1998). There is evidence that volatile general anesthetics interact directly with the transmembrane segments of ligand-gated ion channels (Eckenhoff, 1996a; Mihic et al., 1997). The utility of four-α-helix bundles as models for the transmembrane domains is therefore being explored in an effort to arrive at detailed structural and dynamic descriptions of anesthetic-protein interactions (Johansson et al., 1996, 1998a; Johansson, 1998), with the goal of understanding mechanisms of anesthetic action.

The four-α-helix bundle reported on in the current study, (DesAc-Aα_2-L38M)$_2$, is a variant of the bundle protein (Ac-Aα_2)$_2$ that contains a designed cavity previously shown to improve anesthetic binding affinity (Johansson et al., 1998a). Replacing an α-helical heptad e position leucine with a methionine results in a further increase in the affinity of anesthetic binding. The affinity with which (DesAc-Aα_2-L38M)$_2$ binds halothane is comparable to the clinical EC$_{50}$ of halothane of 250 μM (Franks and Lieb, 1994), raising the

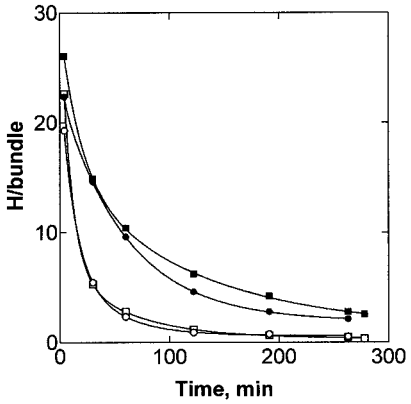

FIGURE 8 Effect of halothane (4.0 mM) on terminal hydrogen exchange rates in the (DesAc-Aα_2-L38M)$_2$ and (DesAc-Aα_2)$_2$ bundles. Open and filled symbols represent, respectively, values measured in the absence and presence of halothane. Squares and circles are data points for the (DesAc-Aα_2-L38M)$_2$ and (DesAc-Aα_2)$_2$ bundles, respectively.

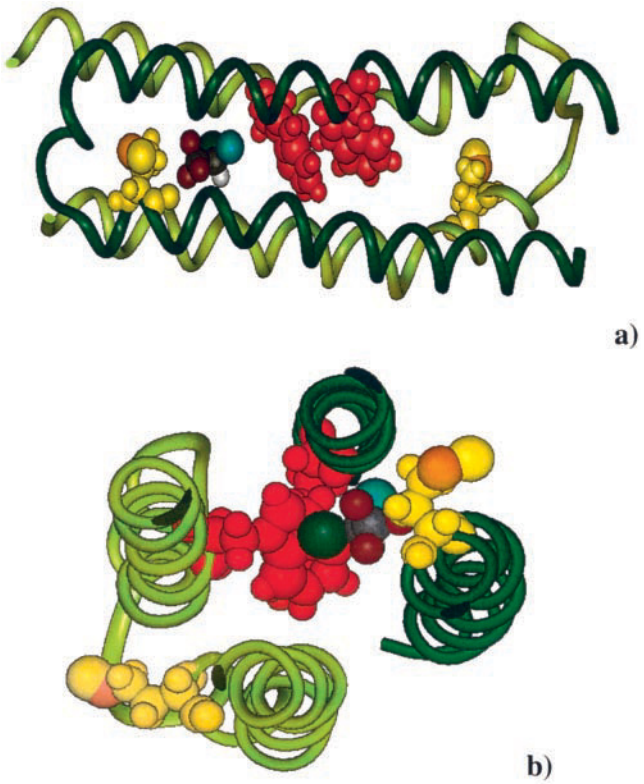

FIGURE 9 The equilibrium structure of the (Ac-Aα_2-L38M)$_2$ bundle with complexed halothane from the constant pressure MD simulation, showing (*a*) a side view and (*b*) a top view at the level of M38. The backbones of the two di-α-helical peptides that dimerize to form a four-α-helix bundle are shown in light and dark green, W15 is in red, and M38 is in yellow, with the sulfur atom in orange. The halothane molecule is shown, with carbon in gray, hydrogen in white, fluorine in brown, chlorine in blue, and bromine in green.

possibility that similar affinity sites may also exist on in vivo protein targets.

To date there have been few direct binding studies using equilibrium approaches to define the energetics of halogenated alkane interactions with proteins. Binding of halothane to bovine serum albumin followed with ^{19}F-NMR spectroscopy (Dubois et al., 1993) and fluorescence quenching (Johansson et al., 1995) resulted in K_d values of 1.3 $\pm$ 0.2 and 1.8 $\pm$ 0.2 mM, respectively. The sites for anesthetic binding on (DesAc-Aα_2-L38M)$_2$ therefore represent the highest affinity binding sites for a volatile anesthetic described so far by an equilibrium binding approach and represent a severalfold increase in affinity compared to the binding sites on bovine serum albumin.

The sites in (DesAc-Aα_2-L38M)$_2$ bind halothane with a K_d = 0.20 $\pm$ 0.01 mM, as determined by the quenching of W15 fluorescence. This corresponds to a 3.5-fold increase in the affinity for the anesthetic compared to the parent four-α-helix bundle with only the designed cavity (Ac-Aα_2)$_2$ (K_d = 0.71 $\pm$ 0.04 mM) (Johansson et al., 1998a). The effect of the leucine-for-methionine substitution on the affinity of anesthetic binding might be explained by 1) a further optimization of cavity size allowing for improved van der Waals interactions, 2) a favorable electrostatic contribution from the nucleophilic methionine sulfur atom, or 3) improved access to the cavity (on rate). A further optimization of cavity size might follow from the greater flexibility of the methionine side chain compared to leucine (Bernstein et al., 1989; O'Neil and DeGrado, 1990b; Gellman, 1991). Leucine tends to adopt one of two low-energy conformations in an α-helical framework (McGregor et al., 1987), while the methionine χ^3 torsion angle distributes over the entire range of possibilities (Janin et al., 1978), indicating an absence of a preferred orientation. This raises the possibility that the methionine residue may interact directly with the bound anesthetic. This interpretation is supported by 1) the decreased W15 fluorescence yield of the (DesAc-Aα_2-L38M)$_2$ bundle compared to the (DesAc-Aα_2)$_2$ bundle, which suggests that the methionine side chain is located within 7 Å of the indole ring (Yuan et al., 1998); 2) the photolabeling results shown in Fig. 7, which suggest that halothane is better coordinated in the (DesAc-Aα_2-L38M)$_2$ bundle compared to the (DesAc-Aα_2)$_2$ bundle, based upon more dominant labeling of W15; and 3) the initial molecular dynamics simulation results (Fig. 9). The photoactivatable end of halothane at the C-Br bond, together with the probable heavy atom perturbation mechanism of fluorescence quenching, indicates orientation of this end of the anesthetic toward the indole ring. This would suggest that the -CF_3 end of halothane could be interacting with the methionine sulfur atom. The sulfur atom on methionine is considerably more polarizable (1.7-fold) than a corresponding -CH_2- group on leucine (Fersht and Dingwall, 1979). This implies that the predicted dispersion forces that underlie volatile general anesthetic binding to proteins (Eckenhoff and Johansson, 1997) will be enhanced,

because the magnitude of these forces is proportional to the polarizabilities of the interacting groups. Support for this interpretation is provided by the finding (Johansson and Zou, 1999) that halothane dissolves 5.2 times better in ethyl methyl sulfide (a model for methionine) than in hexane (a model for leucine). Alternatively, the flexibility of the methionine side chain may translate into improved access to the binding site in the hydrophobic core of the four-α-helix bundle (DesAc-Aα_2-L38M)$_2$. A 3.5-fold increase in the on rate would result in the determined improvement in affinity of (DesAc-Aα_2-L38M)$_2$ for halothane compared to (DesAc-Aα_2)$_2$. However, improved access to the hydrophobic core would also be expected to be accompanied by a decrease in the bundle stability, which is not supported by either the GndCl denaturation experiments or the hydrogen exchange results. An additional possibility is that *two* anesthetic molecules, rather than one, are accommodated in the hydrophobic core of the (DesAc-Aα_2-L38M)$_2$ bundle secondary to allosteric modulation of the dimensions of the binding site by the methionine substitution. In agreement with this are the molecular dynamics results for the (Ac-Aα_2-L38M)$_2$ bundle, which suggest that the hydrophobic pocket is large enough to accommodate two halothane molecules. Further high-resolution structural studies using NMR spectroscopy or x-ray crystallography will be required to definitively address these alternative explanations.

The fluorescence quenching results indicate that halothane binds to the (DesAc-Aα_2-L38M)$_2$ bundle in close proximity to the W15 residues. This follows because heavy atom perturbation, the presumed mode by which halothane quenches tryptophan fluorescence, is a short-range phenomenon, occurring over distances of less than 3–5 Å (Tsao et al., 1989; Basu et al., 1993). The results obtained using direct photoaffinity labeling followed by microsequencing of the bundle protein provide support for this view. Similar complementary results have been reported for the model mammalian protein bovine serum albumin, where fluorescence quenching suggested that the halothane bound in close proximity to the two tryptophan residues W134 and W212 (Johansson et al., 1995) and photoaffinity labeling showed that these two residues were indeed preferentially labeled after halothane photolysis (Eckenhoff, 1996b). This indicates that there is good agreement between the two methods for determining the general location of halothane-binding sites within the protein matrix.

The hydrogen exchange results suggest that halothane binding stabilizes the native folded conformations of the four-α-helix bundles. This is in agreement with prior studies on the (Ac-Aα_2)$_2$ four-α-helix bundle (Johansson, 1998) and on bovine serum albumin (Eckenhoff, 1998; Johansson et al., 1999) and adds further support for the hypothesis that volatile general anesthetics may alter protein function by perturbing the equilibrium between different protein conformations.

The molecular dynamics simulations of the solvated four-α-helix bundles (Ac-Aα_2)$_2$ and (Ac-Aα_2-L38M)$_2$ indicate that both structures are stable and primarily α-helical, in agreement with the CD results. Localization of A8, F12, and W15 within the hydrophobic core in the averaged structures is in accord with the photolabeling results. Residue 38 is observed to support part of the hydrophobic core near W15, which is the proposed site for anesthetic binding (Fig. 9). Examination of the initial results for halothane dynamics in the hydrophobic pocket (Davies et al., 1999b) suggests that it is plausible for a single halothane molecule to satisfy the spatial proximity to W15 required for fluorescence quenching. Halothane is also found to exhibit both rotational and translational motions in the binding pocket (Davies et al., 1999b), which, coupled with the dynamics of the W15 and M38 side chains, allows for effective fluorescence quenching by the bound anesthetic. Structural differences between the (Ac-Aα_2)$_2$ and (Ac-Aα_2-L38M)$_2$ bundles complexed with halothane cannot be inferred at this point but are predicted to play a role in the enhanced binding specificity displayed by the latter. Simulations addressing these issues are currently being performed.

In summary, synthetic peptides are allowing predictions to be made concerning the structural makeup of in vivo general anesthetic binding sites and have enabled a direct test of the hypothesis that the clinical EC_{50} for halothane (250 μM) might correspond to the K_d of a single protein target. It should be noted, however, that a clinical EC_{50} value is unlikely to correspond to the K_d of a binding site on a protein, because the relationship between the ligand concentration that produces a functional effect and the target dissociation constant is often shifted (Eckenhoff and Johansson, 1997). However, higher affinity sites are more likely to be occupied by an anesthetic molecule than lower affinity sites, at clinical concentrations. Taken together, the results with these simple models suggest that volatile general anesthetics are likely to occupy preexisting appropriately sized hydrophobic cavities on proteins and that the presence of methionine and aromatic residues lining the cavity favors anesthetic binding. The small size of these protein bundles will permit the structural and dynamic consequences of anesthetic binding to be probed through detailed biophysical approaches and MD simulations. For example, one of the consequences of a bound volatile general anesthetic that has been explored recently is the effect on global protein stability as reported here and previously (Johansson, 1998; Eckenhoff, 1998; Johansson et al., 1999). Thus stabilization of the native, folded protein by a bound anesthetic molecule may prevent the conformational changes required for protein function, perhaps representing a fundamental mechanism of volatile anesthetic action.

Mass spectrometry and protein microsequencing were performed by the Protein Chemistry Laboratory, University of Pennsylvania, Philadelphia,

PA. We thank Dr. Brian R. Gibney and Prof. Michael L. Klein for helpful discussions.

This work was supported by National Institutes of Health grants GM55876 and GM51595 and a FAER Young Investigator Award. Computer resources for this work were provided by the San Diego Supercomputer Center (MCA93S020) and the Pittsburgh Supercomputer Center (CHE980006P). This paper was presented in part at the annual meeting of the American Society of Anesthesiologists, Orlando, FL, October 1998.

REFERENCES

Ballew, R. M., J. Sabelko, and M. Gruebele. 1996. Direct observation of fast protein folding: the initial collapse of apomyoglobin. *Proc. Natl. Acad. Sci. USA.* 93:5759–5764.

Basu, G., D. Anglos, and A. Kuki. 1993. Fluorescence quenching in a strongly helical peptide series: the role of noncovalent pathways in modulating electronic interactions. *Biochemistry.* 32:3067–3076.

Bernstein, H. D., M. A. Poritz, K. Strub, P. J. Hoben, S. Brenner, and P. Walter. 1989. Model for signal sequence recognition from amino-acid sequence of 54k subunit of signal recognition particle. *Nature.* 340: 482–486.

Betz, S. F., P. A. Liebman, and W. F. DeGrado. 1997. De novo design of native proteins: characterization of proteins intended to fold into antiparallel, Rop-like, four-helix bundles. *Biochemistry.* 36:2450–2458.

Bryson, J. W., S. F. Betz, H. S. Lu, D. J. Suich, H. X. Zhou, K. T. O'Neil, and W. F. DeGrado. 1995. Protein design: a hierarchic approach. *Science.* 270:935–941.

Cantor, R. 1997. The lateral pressure profile in membranes: a physical mechanism of general anesthesia. *Biochemistry.* 36:2339–2344.

Cornell, W. D., P. Cieplak, C. I. Bayly, I. R. Gould, K. M. Merz, D. M. Ferguson, D. C. Spellmeyer, T. Fox, J. W. Caldwell, and P. A. Kollman. 1995. A second generation force field for the simulation of proteins and nucleic acids. *J. Am. Chem. Soc.* 117:5179–5197.

Davies, L. A., M. L. Klein, and D. Scharf. 1999a. The vacuum structure of a synthetic four-α-helix bundle which binds halothane. *Biophys. J.* 76:A383.

Davies, L. A., M. L. Klein, and D. Scharf. 1999b. Molecular dynamics simulation of a synthetic four-α-helix bundle that binds the anesthetic halothane. *FEBS Lett.* 455:332–338.

Dougherty, D. A. 1996. Cation-π interactions in chemistry and biology: a new view of benzene, Phe, Tyr, and Trp. *Science.* 271:163–168.

Doyle, D. A., J. Morais Cabral, R. A. Pfuetzner, A. Kuo, J. M. Gulbis, S. L. Cohen, B. T. Chait, and R. MacKinnon. 1998. The structure of the potassium channel: molecular basis of K^+ conduction and selectivity. *Science.* 280:69–77.

Dubois, B. W., S. F. Cherian, and A. S. Evers. 1993. Volatile anesthetics compete for common binding sites on bovine serum albumin: a ^{19}F-NMR study. *Proc. Natl. Acad. Sci. USA.* 90:6478–6482.

Dubois, B. W., and A. S. Evers. 1992. ^{19}F-NMR spin-spin relaxation (T_2) method for characterizing anesthetic binding to proteins: analysis of isoflurane binding to albumin. *Biochemistry.* 31:7069–7076.

Eckenhoff, R. G. 1996a. An inhalational anesthetic binding domain in the nicotinic acetylcholine receptor. *Proc. Natl. Acad. Sci. USA.* 93: 2807–2810.

Eckenhoff, R. G. 1996b. Amino acid resolution of halothane binding sites in serum albumin. *J. Biol. Chem.* 271:15521–15526.

Eckenhoff, R. G. 1998. Do specific or nonspecific interactions with proteins underlie inhalational anesthetic action. *Mol. Pharmacol.* 54: 610–615.

Eckenhoff, R. G., and J. S. Johansson. 1997. Interactions between inhaled anesthetics and proteins. *Pharmacol. Rev.* 49:343–367.

Eckenhoff, R. G., and H. Shuman. 1993. Halothane binding to soluble proteins determined by photoaffinity labeling. *Anesthesiology.* 79: 96–106.

Edelhoch, H. 1967. Spectroscopic determination of tryptophan and tyrosine in proteins. *Biochemistry.* 6:1948–1954.

Fersht, A. R., and C. Dingwall. 1979. Cysteinyl-tRNA synthetase from *Escherichia coli* does not need an editing mechanism to reject serine and alanine. High binding energy of small groups in specific molecular interactions. *Biochemistry.* 18:1245–1249.

Franks, N. P., and W. R. Lieb. 1994. Molecular and cellular mechanisms of general anesthesia. *Nature.* 367:607–614.

Gellman, S. H. 1991. On the role of methionine residues in the sequence-independent recognition of nonpolar protein surfaces. *Biochemistry.* 30:6633–6636.

Gibney, B. R., J. S. Johansson, F. Rabanal, J. J. Skalicky, A. J. Wand, and P. L. Dutton. 1997a. Global topology and stability and local structure and dynamics in a synthetic spin-labeled four-helix bundle protein. *Biochemistry.* 36:2798–2806.

Gibney, B. R., S. E. Mulholland, F. Rabanal, and P. L. Dutton. 1996. Ferredoxin and ferredoxin-heme maquettes. *Proc. Natl. Acad. Sci. USA.* 93:15041–15046.

Gibney, B. R., F. Rabanal, J. J. Skalicky, A, J. Wand, and P. L. Dutton. 1997b. Design of a unique protein scaffold for maquettes. *J. Am. Chem. Soc.* 119:2323–2324.

Harris, R. A., S. J. Mihic, J. E. Dildy-Mayfield, and T. K. Machu. 1995. Actions of anesthetics on ligand-gated ion channels: role of receptor subunit composition. *FASEB J.* 9:1454–1462.

Janin, J., S. Wodak, M. Levitt, and B. Maigret. 1978. Conformation of amino acid side-chains in proteins. *J. Mol. Biol.* 125:357–386.

Jasanoff, A., and A. R. Fersht. 1994. Quantitative determination of helical propensities from trifluoroethanol titration curves. *Biochemistry.* 33: 2129–2135.

Jevtovic-Todorovic, V., S. M. Todorovic, S. Mennerick, S. Powell, K. Dikranian, N. Benshoff, C. F. Zorumski, and J. W. Olney. 1998. Nitrous oxide (laughing gas) is an NMDA antagonist, neuroprotectant and neurotoxin. *Nature Med.* 4:460–463.

Johansson, J. S. 1997. Binding of the volatile anesthetic chloroform to albumin demonstrated using tryptophan fluorescence quenching. *J. Biol. Chem.* 272:17961–17965.

Johansson, J. S. 1998. Probing the structural features of volatile anesthetic binding sites with synthetic peptides. *Toxicol. Lett.* 101:369–375.

Johansson, J. S., R. G. Eckenhoff, and P. L. Dutton. 1995. Binding of halothane to serum albumin demonstrated using tryptophan fluorescence. *Anesthesiology.* 83:316–324.

Johansson, J. S., B. R. Gibney, F. Rabanal, K. S. Reddy, and P. L. Dutton. 1998a. A designed cavity in the hydrophobic core of a four-α-helix bundle improves volatile anesthetic binding affinity. *Biochemistry.* 37: 1421–1429.

Johansson, J. S., B. R. Gibney, J. J. Skalicky, A. J. Wand, and P. L. Dutton. 1998b. A native-like three-α-helix bundle protein from structure based redesign: a novel maquette scaffold. *J. Am. Chem. Soc.* 120:3881–3886.

Johansson, J. S., F. Rabanal, and P. L. Dutton. 1996. Binding of the volatile anesthetic halothane to the hydrophobic core of a tetra-α-helix bundle protein. *J. Pharmacol. Exp. Ther.* 279:56–61.

Johansson, J. S., and H. Zou. 1999. Partitioning of four modern volatile general anesthetics into solvents that model buried amino acid side-chains. *Biophys. Chem.* 79:107–116.

Johansson, J. S., H. Zou, and J. T. Tanner. 1999. Bound volatile general anesthetics alter both local protein dynamics and global protein stability. *Anesthesiology.* 90:235–245.

Jorgensen, W. L., J. D. Chandrasekhar, J. D. Madura, R. W. Impey, and M. L. Klein. 1983. Comparison of simple potential functions for simulating liquid water. *J. Chem. Phys.* 79:926–935.

Lau, S. Y. M., A. K. Taneja, and R. S. Hodges. 1984. Synthesis of a model protein of defined secondary and quaternary structure. *J. Biol. Chem.* 259:13253–13261.

Martyna, G. L., M. E. Tuckerman, D. J. Tobias, and M. L. Klein. 1996. Explicit reversible integrators for extended systems dynamics. *Mol. Physiol.* 87:1117–1157.

McGregor, M. J., S. A. Islam, and M. J. Sternberg. 1987. Analysis of the relationship between side-chain conformation and secondary structure in globular proteins. *J. Mol. Biol.* 198:295–310.

Mihic, S. J., Q. Ye, M. J. Wick, V. V. Koltchine, M. D. Krasowski, S. E. Finn, M. P. Mascia, C. F. Valenzuela, K. K. Hanson, E. P. Greenblatt, R. A. Harris, and N. L. Harrison. 1997. Sites of alcohol and volatile anaesthetic action on $GABA_A$ and glycine receptors. *Nature.* 389: 385–389.

Mok, Y-K., G. De Prat Gay, J. P. Butler, and M. Bycroft. 1996. Equilibrium dissociation and unfolding of the dimeric human papillomavirus strain-16 E2 DNA- binding domain. *Protein Sci.* 5:310–319.

Nozaki, Y., and C. Tanford. 1971. The solubility of amino acids and two glycine peptides in aqueous ethanol and dioxane solutions. *J. Biol. Chem.* 246:2211–2217.

O'Neil, K. T., and W. F. DeGrado. 1990a. A thermodynamic scale for the helix-forming tendencies of the commonly occurring amino acids. *Science.* 250:646–651.

O'Neil, K. T., and W. F. DeGrado. 1990b. How calmodulin binds its targets: sequence independent recognition of amphiphilic α-helices. *Trends Biochem. Sci.* 15:59- 64.

Rabanal, F., W. F. DeGrado, and P. L. Dutton. 1996. Toward the synthesis of a photosynthetic reaction center maquette: a cofacial porphrin pair assembled between two subunits of a synthetic four-helix bundle multiheme protein. *J. Am. Chem. Soc.* 118:473–474.

Rees, D. C., H. Komiya, T. O. Yeates, J. P. Allen, and G. Feher. 1989. The bacterial photosynthetic reaction center as a model for membrane proteins. *Annu. Rev. Biochem.* 58:607–633.

Richards, F. M. 1974. The interpretation of protein structures: total volume, group volume distributions and packing density. *J. Mol. Biol.* 82:1–14.

Robertson, D. E., R. S. Farid, C. C. Moser, J. L. Urbauer, S. E. Mulholland, R. Pidikiti, J. D. Lear, A. J. Wand, W. F. DeGrado, and P. L. Dutton. 1994. Design and synthesis of multi-haem proteins. *Nature.* 368: 425–432.

Shibata, A., K. Morita, T. Yamashita, H. Kamaya, and I. Ueda. 1991. Anesthetic-protein interaction: effects of volatile anesthetics on the secondary structure of poly(L-lysine). *J. Pharm. Sci.* 80:1037–1041.

Skalicky, J. J., B. R. Gibney, F. Rabanal, R. J. Bieber Urbauer, P. L. Dutton, and A. J. Wand. 1999. Solution structure of a designed four-α-helix bundle maquette scaffold. *J. Am. Chem. Soc.* 121:4941–4951.

Takenoshita, M., and J. H. Steinbach. 1991. Halothane blocks low-voltage-activated calcium current in rat sensory neurons. *J. Neurosci.* 11: 1404–1412.

Tsao, D. H. H., J. R. Casa-Finet, A. H. Maki, and J. W. Chase. 1989. Triplet state properties of tryptophan residues in complexes of mutated *Escherichia coli* single-stranded DNA binding proteins with single-stranded polynucleotides. *Biophys. J.* 55:927–936.

Tu, K., M. Tarek, M. L. Klein, and D. Scharf. 1998. Effects of anesthetics on the structure of a phospholipid bilayer: MD investigation of halothane in the hydrated liquid crystal phase of dipalmitoylphosphatidylcholine. *Biophys. J.* 75:2123–2134.

Urry, D. W., D. C. Gowda, T. M. Parker, C. H. Luan, M. C. Reid, C. M. Harris, A. Pattanaik, and R. D. Harris. 1992. Hydrophobicity scale for proteins based on inverse temperature transitions. *Biopolymers.* 39: 1243–1250.

von Heijne, G. 1994. Membrane proteins: from sequence to structure. *Annu. Rev. Biophys. Biomol. Struct.* 23:167–192.

Weiner, S. J., P. A. Kollman, D. A. Case, U. C. Singh, C. Ghio, G. Alagona, S. Profeta, and P. Weiner. 1984. A new force field for molecular mechanics simulation of nucleic acids and proteins. *J. Am. Chem. Soc.* 106:765–775.

Weiner, S. J., P. A. Kollman, D. T. Nguyen, and D. A. Case. 1986. An all atom force field for simulations of proteins and nucleic acids. *J. Comp. Chem.* 7:230–235.

Wimbley, W. C., and S. H. White. 1996. Experimentally determined hydrophobicity scale for proteins at membrane interfaces. *Nature Struct. Biol.* 3:842–848.

Yuan, T., A. M. Weljie, and H. J. Vogel. 1998. Tryptophan fluorescence quenching by methionine and selenomethionine residues of calmodulin: orientation of peptide and protein binding. *Biochemistry.* 37:3187–3195.

Zhou, N. E., C. M. Kay, and R. S. Hodges. 1992. Synthetic model proteins. Positional effects of interchain hydrophobic interactions on stability of two-stranded α-helical coiled-coils. *J. Biol. Chem.* 267:2664–2670.